

Role of Dispersion and Electrostatic Forces on Solute–Solvent Interactions in a Nematic Liquid Crystal Phase

Vance E. Williams and Robert P. Lemieux*

Contribution from the Department of Chemistry, Queen's University, Kingston, Ontario, Canada K7L 3N6

Received July 31, 1998

Abstract: A series of 23 substituted biphenyl, phenylpyridine, and bipyridine derivatives were doped in the nematic liquid crystal host 4'-(pentyloxy)-4-biphenylcarbonitrile over the mole fraction range $0.005 \leq x_d \leq 0.04$. The effect of each biaryl dopant on the nematic–isotropic phase transition temperature (clearing point) of the liquid crystal phase was determined by differential scanning calorimetry as a function of dopant mole fraction for a wide range of substituents and expressed as a constant of proportionality δ_1 . The molecular polarizability (α) and electrostatic character (E_{HOMO}) of each dopant were estimated using ab initio calculations at the HF/3-21G* level. Analysis of the combined δ_1 data with respect to α and E_{HOMO} by multilinear regression showed that a reasonable correlation exists between δ_1 and a linear combination of α and E_{HOMO} ($R^2 = 0.81$) which represents a statistically significant improvement over correlations between δ_1 and α ($R^2 = 0.72$) and between δ_1 and E_{HOMO} ($R^2 = 0.56$). These results provide evidence that arene–arene interactions in the absence of a ternary solvent are controlled by both electrostatic and dispersion forces. In this work, dispersion forces were shown to strongly influence the stability of the nematic phase, with a secondary influence coming from electrostatic forces. Furthermore, the results suggest that charge-transfer complexation and molecular dipole–dipole interactions do not have an appreciable effect on the stability of arene–arene interactions in the nematic phase.

Introduction

Noncovalent interactions between aromatic rings play a pivotal role in the stabilization of many molecular structures found in biological systems, including the helical structure of DNA¹ and the tertiary structure of proteins,² and in the design of many synthetic host–guest inclusion complexes and supramolecular assemblies.³ Indeed, the tendency of aromatic functional groups to associate in edge-to-face or π -stacked complexes constitutes a basic tool of supramolecular chemistry; exploitation of arene–arene interactions in this context requires a detailed understanding of the forces controlling them. Several

recent experimental^{3a,4} and theoretical⁵ studies suggest that dispersion and electrostatic forces dominate the intermolecular potential of aromatic complexes.

The interpretation of substituent effects can provide valuable insight into the nature of arene–arene interactions and the respective contributions of electrostatic, charge-transfer, and dispersion forces. For example, Cozzi and Siegel recently showed by variable temperature ¹H NMR spectroscopy that the barrier to epimerization of substituted 1,8-di-*o*-tolyl naphthalenes increases with substituents of increasing electron-withdrawing character, which suggests that π -stacked arene–arene interactions are controlled primarily by electrostatic forces.^{4c} Dispersion forces are also believed to play an important role in stabilizing arene–arene complexes,⁶ although few experimental results correlating molecular polarizability with arene–arene binding energies can be found in the literature.^{3d,7} This may be ascribed in part to difficulties in measuring the effect of molecular polarizability on complexes formed in solution due to the “dampening” effect of the solvent.⁸ Mulliken has argued that the contribution of dispersion forces toward complex formation should be negligible in solution because solute–solute dispersion forces are approximately compensated by the loss of solute–solvent dispersive interactions. The extent to which this is true, however, is highly dependent on the polarizability of the solvent.^{9,10}

To avoid the complications associated with the dampening effect of a ternary solvent and investigate the role of both dispersion and electrostatic forces in aromatic complexes, we

* To whom correspondence should be addressed: email:lemieux@chem.queensu.ca.

(1) Saenger, W. *Principles of Nucleic Acid Structure*; Springer-Verlag: Berlin, 1984.

(2) Burley, S. K.; Petsko, G. A. *Science* **1985**, 229, 23.

(3) (a) Muehldorf, A. V.; Van Engen, D.; Warner, J. C.; Hamilton, A. D. *J. Am. Chem. Soc.* **1988**, 110, 6562. (b) Pirkle, W. H.; Pochapsky, T. C. *Chem. Rev.* **1989**, 89, 347. (c) Rebek, J. *Angew. Chem., Int. Ed. Engl.* **1990**, 29, 245. (d) Ferguson, S. B.; Sanford, E. M.; Seward, E. M.; Diederich, F. *J. Am. Chem. Soc.* **1991**, 113, 5410. (e) Zimmerman, S. *Topics in Current Chemistry*; Springer-Verlag: Berlin, 1993; Vol. 165, p 72. (f) Amabilino, D. B.; Stoddard, J. F. *Chem. Rev.* **1995**, 95, 2725.

(4) (a) Hunter, C. A. *Chem. Soc. Rev.* **1994**, 101. (b) Philip, D.; Gramlich, V.; Seiler, P.; Diederich, F. *J. Chem. Soc., Perkin Trans. 2* **1995**, 875. (c) Cozzi, F.; Siegel, J. S. *Pure Appl. Chem.* **1995**, 67, 683. (d) Shetty, A. S.; Zhang, J.; Moore, J. S. *J. Am. Chem. Soc.* **1996**, 118, 1019. (e) Williams, V. E.; Lemieux, R. P. *Chem. Commun.* **1996**, 2259. (f) Carver, F. J.; Hunter, C. A.; Seward, E. M. *Chem. Commun.* **1998**, 775.

(5) (a) Price, S. L.; Stone, A. J. *J. Phys. Chem.* **1987**, 86, 2859. (b) Glauser, W. A.; Raber, D. J.; Stevens, B. *J. Chem. Phys.* **1989**, 93, 1784. (c) Hunter, C. A.; Sanders, J. K. M. *J. Am. Chem. Soc.* **1990**, 112, 5525. (d) Jorgensen, W. L.; Severance, D. L. *J. Am. Chem. Soc.* **1990**, 112, 4768. (e) Hobza, P.; Selzle, H. L.; Schlag, E. W. *Chem. Rev.* **1994**, 94, 4, 1767. (f) Williams, V. E.; Lemieux, R. P.; Thatcher, G. R. J. *J. Org. Chem.* **1996**, 61, 1, 1927. (g) Castro, R.; Berardi, M. J.; Cordova, E.; Ochoa de Olza, M.; Kaifer, A. E.; Evanseck, J. D. *J. Am. Chem. Soc.* **1996**, 118, 10257.

(6) Dewar, M. J. S.; Thompson, C. C. *Tetrahedron Suppl.* **1966**, 7, 97.

(7) Williams, K.; Askew, B.; Ballester, P.; Buhr, C.; Jeong, K. S.; Jones, S.; Rebek, J. *J. Am. Chem. Soc.* **1989**, 111, 1090.

(8) Mulliken, R. S.; Person, W. B. *Molecular Complexes: A Lecture and Reprint Volume*; Wiley-Interscience: New York, 1969.

have undertaken a systematic study of arene–arene interactions between substituted aromatic solutes (dopants) and aromatic liquid crystal solvents through measurements of dopant-induced perturbations in the bulk properties of the liquid crystal phase. For instance, we have recently shown that the propensity of a series of atropisomeric dibenzoxepin dopants to induce a chiral nematic (cholesteric) liquid crystal phase varies with the electron-withdrawing character (σ_p) and polarizability (α) of substituents on the chiral dopant.^{4e} Given the assumption that cholesteric induction takes place via chiral conformational interactions that are π -facial in nature, these results provide further evidence that π -stacking complexes are controlled primarily by dispersion and electrostatic forces. As an extension of this work, we have investigated substituent effects on arene–arene interactions in a nematic liquid crystal in the absence of any conformational restriction, which allows us to probe π -stacking as well as edge-to-face interactions between orientationally ordered systems. This has been achieved by doping a cyanobiphenyl nematic liquid crystal with a series of substituted biaryl dopants and measuring the corresponding changes in nematic–isotropic phase transition temperature (clearing point) as a function of dopant concentration.

The introduction of a dopant in a liquid crystal host generally causes a shift in the clearing point (T_{NI}) that is a function of dopant–host interactions. At low dopant mole fraction (i.e., $x_d < 0.05$), dopant–dopant interactions are negligible and T_{NI} varies linearly with x_d according to eq 1, where T_{NI}° is the clearing point of the pure liquid crystal host and δ_1 is a proportionality constant in kelvins that constitutes a measure of the propensity of the dopant to stabilize (positive δ_1) or destabilize (negative δ_1) the liquid crystal phase.¹¹ In this paper, we report the measurement of δ_1 values for a series of substituted biaryl dopants 1–6 in the cyanobiphenyl nematic liquid crystal **5OCB**, and the correlation of these values with the molecular polarizability and electrostatic character of the dopants derived from ab initio calculations at the HF/3-21G* level of theory.

$$T_{NI} = T_{NI}^\circ + \delta_1 x_d \quad (1)$$

Experimental Section

Materials. The nematic liquid crystal host 4'-(pentyloxy)-4-biphenylcarbonitrile (**5OCB**) was purchased from Aldrich and used without further purification. Biphenyl (**1a**), 4,4'-dibromobiphenyl (**1d**), 4-methylbiphenyl (**2b**), 4-acetoxypiphenyl (**2e**), 4-nitrobiphenyl (**2f**), decafluorobiphenyl (**4**), 4-phenylpyridine (**5**), and 4,4'-bipyridine (**6**) were purchased from Aldrich. Compounds **1a**, **2b**, and **2f** were recrystallized from EtOH; the others were used without further purification. 4,4'-Difluorobiphenyl (**1b**),¹² 4,4'-dichlorobiphenyl (**1c**),¹³ 4,4'-diiodobiphenyl (**1e**),¹⁴ 4,4'-dimethylbiphenyl (**1f**),¹⁵ 4,4'-dimethoxy-

(9) The de Boer–Hamaker theorem describes the dispersion component of the complexation energy of two solute molecules *a* and *b* in a solvent *s* as $E_{ab}(\text{solution}) = E_{ab} + E_{ss} - E_{as} - E_{bs}$, where E_{ab} , E_{as} , E_{bs} , and E_{ss} are the gas phase energies of solute–solute, solute–solvent, and solvent–solvent interactions, respectively: Hamaker, H. C. *Physica*, **1937**, 4, 1058. If one assumes that relative values of these terms are approximately proportional to the molecular polarizabilities of the constituent molecules, then Mulliken's condition of no net gain in dispersion forces holds when $\alpha_a \alpha_b \approx \alpha_s$.

(10) For example, the binding constant of an inclusion complex formed by a macrobicyclic cyclophane host and pyrene has been shown to decrease with solvents of increasing polarizability: Smithrud, D.; Diederich, F. *J. Am. Chem. Soc.* **1990**, 112, 339.

(11) Kobayashi, M.; Maeda, A.; Tanizaki, Y.; Okuba, J.; Hushi, T. *Chem. Lett.* **1988**, 557.

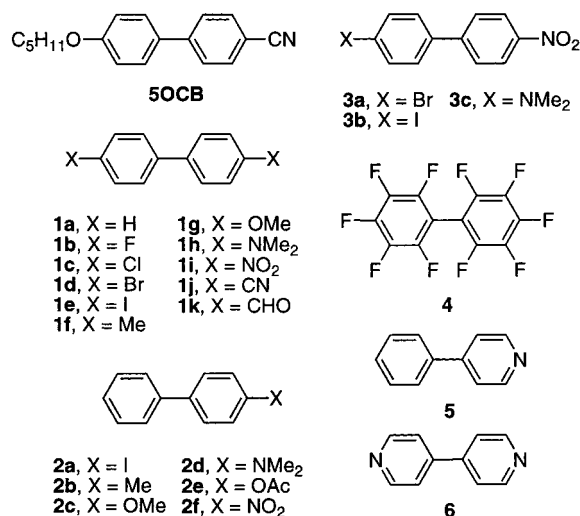
(12) Schiemann, G.; Winkelmüller, W. *Organic Syntheses*; Wiley: New York, 1942; Collect. Vol. 2, p 188.

(13) Schwechten, H.-W. *Chem. Ber.* **1932**, 65, 1605.

(14) Ibuki, E.; Ozasa, S.; Murai, K. *Bull. Chem. Soc. Jpn.* **1975**, 48, 1868.

(15) Kharash, M. S.; Fields, E. K. *J. Am. Chem. Soc.* **1941**, 63, 2316.

Scheme 1



biphenyl (**1g**),¹⁶ *N,N,N',N'*-tetramethylbenzidine (**1h**),¹⁷ 4,4'-dinitrobiphenyl (**1i**),¹⁸ 4,4'-dicyanobiphenyl (**1j**),¹⁹ 4,4'-diformylbiphenyl (**1k**),²⁰ 4-iodobiphenyl (**2a**),¹⁴ 4-methoxybiphenyl (**2c**),¹⁶ 4-(*N,N*-dimethylamino)biphenyl (**2d**),¹⁷ 4-bromo-4'-nitrobiphenyl (**3a**),¹⁶ 4-iodo-4'-nitrobiphenyl (**3b**),²¹ and 4-(*N,N*-dimethylamino)-4'-nitrobiphenyl (**3c**)¹⁷ were prepared by literature procedures and shown to have the expected physical and spectral properties.

DSC Measurements. DSC measurements were performed with a Perkin-Elmer DSC7 differential scanning calorimeter at a scanning rate of 5 K/min using helium as the purge gas. The instrument was calibrated before each session with indium. To minimize error arising from drift in the calibration, endotherms for all mixtures of a given dopant were recorded in immediate succession, along with the endotherm for a neat sample of **5OCB**. The same sample of neat **5OCB** was used as a reference for all mixtures.

Calculations. All structures were built and geometry optimized at the HF/3-21G* level using the Spartan 4.0 molecular modeling program.²² Optimized Cartesian coordinates were then used to calculate molecular polarizabilities with the HF/3-21G* basis set implemented in Gaussian 94 using the "polar" keyword.²³ Calculations were performed on a RISC-based IBM SP2 parallel processing computer.

Results and Discussion

DSC Measurements. The compound **5OCB** was selected as the liquid crystal host because it exhibits a broad nematic phase between 321 and 340 K, which allows the measurement of relatively large negative ΔT_{NI} values ($T_{NI} - T_{NI}^\circ$) above room temperature. The symmetrical and unsymmetrical 4,4'-disubstituted biphenyls **1–3**, decafluorobiphenyl (**4**), 4-phenylpyridine (**5**), and 4,4'-bipyridine (**6**) were used as dopants. Mixtures of each dopant in the host **5OCB** were prepared at three different x_d values between 0.005 and 0.04, and T_{NI} values were measured by differential scanning calorimetry on heating from 303 to 348

(16) Gray, G. W.; Hartley, J. B.; Jones, B. *J. Chem. Soc.* **1955**, 1412.

(17) Burch, R. F. *J. Org. Chem.* **1972**, 37, 1673.

(18) Gull, H. C.; Turner, E. E. *J. Chem. Soc.* **1929**, 491.

(19) Friedman, L.; Shecter, H. *J. Org. Chem.* **1961**, 26, 2522.

(20) Helms, A.; Heiler, D.; McLendon, G. *J. Am. Chem. Soc.* **1992**, 114, 6227.

(21) Belcher, R.; Nutten, A. J.; Stephen, W. I. *J. Chem. Soc.* **1953**, 1953, 1334.

(22) Wavefunctions, Inc.: 18401 Von Karmann, #210, Irvine, CA.

(23) Gaussian 94: Rev. B.3; M. J. Frisch, G. W. Trucks, H. B. Schlegel, P. M. W. Gill, B. G. Johnson, M. A. Robb, J. R. Cheeseman, T. Keith, G. A. Petersson, J. A. Montgomery, K. Raghavachari, M. A. Al-Laham, V. G. Zakrzewski, J. V. Ortiz, J. B. Foresman, C. Y. Peng, P. Y. Ayala, W. Chen, M. W. Wong, J. L. Andres, E. S. Replogle, R. Gomperts, R. L. Martin, D. J. Fox, J. S. Binkley, D. J. Defrees, J. Baker, J. P. Stewart, M. Head-Gordon, C. Gonzalez, and J. A. Pople, Gaussian, Inc.: Pittsburgh, PA, 1995.

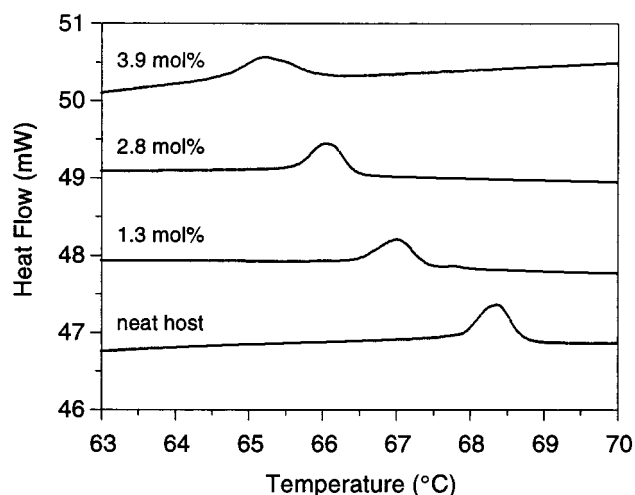


Figure 1. DSC endotherms at the nematic–isotropic phase transition for the nematic host **5OCB** and for mixtures of dopant **1b** in the nematic host **5OCB** at three different mole fractions: $x_d = 0.013$, 0.028, and 0.039.

Table 1. Experimental δ_1 Values for the Symmetrical Dopants **1**, **4**, and **6** in the Nematic Host **5OCB** and Calculated Values of the Dopant Polarizabilities (α) and HOMO and LUMO Energies at the HF/3-21G* Level

| dopant | X | δ_1 (K) | α (esu) | E_{HOMO} (hartrees) | E_{LUMO} (hartrees) |
|-----------|------------------|----------------|----------------|------------------------------|------------------------------|
| 1a | H | -114 ± 25 | 102.9 | -0.311 | 0.120 |
| 1b | F | -74 ± 6 | 101.3 | -0.323 | 0.113 |
| 1c | Cl | -69 ± 9 | 127.0 | -0.323 | 0.096 |
| 1d | Br | -46 ± 16 | 132.6 | -0.316 | 0.097 |
| 1e | I | -52 ± 9 | 151.9 | -0.311 | 0.093 |
| 1f | Me | -16 ± 3 | 127.8 | -0.297 | 0.125 |
| 1g | OMe | $+13 \pm 5$ | 134.4 | -0.284 | 0.136 |
| 1h | NMe ₂ | $+139 \pm 18$ | 167.9 | -0.244 | 0.153 |
| 1i | NO ₂ | -62 ± 14 | 133.1 | -0.370 | 0.014 |
| 1j | CN | $+21 \pm 6$ | 134.5 | -0.344 | 0.054 |
| 1k | CHO | -55 ± 12 | 131.8 | -0.335 | 0.055 |
| 4 | | -196 ± 30 | 99.0 | -0.396 | 0.048 |
| 6 | | -188 ± 2 | 92.4 | -0.362 | 0.087 |

Table 2. Experimental δ_1 Values for the Unsymmetrical Dopants **2**, **3**, and **5** in the Nematic Host **5OCB**, and Calculated Values of the Dopant Polarizabilities (α) and HOMO and LUMO Energies at the HF/3-21G* Level

| dopant | X | δ_1 (K) | α (esu) | E_{HOMO} (hartrees) | E_{LUMO} (hartrees) |
|-----------|------------------|----------------|----------------|------------------------------|------------------------------|
| 2a | I | -72 ± 8 | 126.8 | -0.310 | 0.105 |
| 2b | Me | -85 ± 1 | 115.3 | -0.303 | 0.122 |
| 2c | OMe | -52 ± 12 | 118.6 | -0.294 | 0.127 |
| 2d | NMe ₂ | -16 ± 2 | 135.3 | -0.264 | 0.135 |
| 2e | OAc | -101 ± 8 | 128.0 | -0.307 | 0.117 |
| 2f | NO ₂ | -84 ± 21 | 118.5 | -0.338 | 0.040 |
| 3a | Br | -62 ± 16 | 133.5 | -0.337 | 0.034 |
| 3b | I | -44 ± 3 | 143.0 | -0.330 | 0.034 |
| 3c | NMe ₂ | $+8 \pm 5$ | 154.5 | -0.281 | 0.047 |
| 5 | | -156 ± 13 | 97.7 | -0.362 | 0.087 |

K. A representative series of DSC endotherms at the nematic–isotropic phase transition is shown in Figure 1 for **1b/5OCB** mixtures. In each case, T_{NI} was taken as the highest point on the endotherm peak. Values of δ_1 were obtained for each dopant via linear regression analysis by plotting T_{NI} vs x_d . These values are listed in Tables 1 and 2 along with standard errors derived from the regression analyses. In all cases, the expected linear relation between x_d and T_{NI} was observed over the concentration range examined.

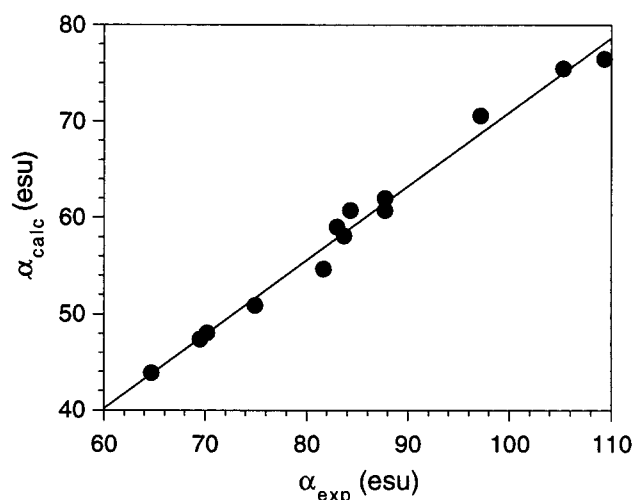


Figure 2. Plot of calculated polarizabilities (α_{calc}) at the HF/3-21G* level versus experimental polarizabilities (α_{exp}) for pyridine and a series of monosubstituted benzenes (X = H, F, Cl, CN, Me, NO₂, OH, OMe, NH₂, NMe₂, SMe, CH=CH₂); $R^2 = 0.99$.

Molecular Polarizability of the Dopants. Previous work by Bursi et al. has shown that ab initio calculations of molecular polarizabilities (α) for homologous series of aromatic compounds reproduce experimental trends accurately, with virtually no dependence on the basis set used.²⁴ In this case, molecular polarizabilities were calculated for all molecules at the HF/3-21G* level.²⁵ The suitability of this basis set to reproduce experimental trends in the series **1–6** was confirmed by calculating α values for a series of monosubstituted benzenes and plotting the results against the experimental α values derived from the Lorenz–Lorentz equation,²⁶ as shown in Figure 2. Although these results show that the 3-21G* basis set systematically underestimates molecular polarizability, this level of theory provides relative α values that are reliable enough to study the relative contribution of molecular polarizability to δ_1 . The calculated α values for dopants **1–6** are listed in Tables 1 and 2.

Electrostatic Character of the Dopants. The relative electrostatic character of compounds in series **1–3** can be adequately described by the sum of Hammett σ_p constants for substituents X.^{4c} However, this approach cannot be used for compounds **4**, **5**, and **6** due to the lack of Hammett parameters for such systems. An alternative approach to this problem, which is consistent with the computational approach used for α values, is to estimate the relative electrostatic character of all dopants based on calculated HOMO energies. These values are readily available from the HF/3-21G* calculations used to determine α values, and we have found a good correlation between calculated E_{HOMO} and σ_p constants for a series of monosubstituted benzenes, as shown in Figure 3. E_{HOMO} and E_{LUMO} values were calculated for all dopants and for the host **5OCB** and are listed in Tables 1 and 2.

Correlation of Molecular Parameters with δ_1 . Analysis of the data in Tables 1 and 2 for dopants **1–6** showed that some correlation exists between δ_1 and E_{HOMO} ($R^2 = 0.56$), as shown in Figure 4. The stability of the liquid crystal phase was found to increase with the electron-donating character of X. At one

(24) Bursi, R.; Lankhorst, M.; Feil, D. *J. Comput. Chem.* **1995**, *16*, 545.

(25) Molecular polarizabilities are determined in Gaussian 94 by analytically solving for the second derivative of energy with respect to an external electric field.

(26) Zeegers-Huyskens, T.; Huyskens, P. L. In *Intermolecular Forces*; Huyskens, P. L., Luck, W. A. P., Zeegers-Huyskens, T., Eds.; Springer-Verlag: Berlin, 1991; p 5.

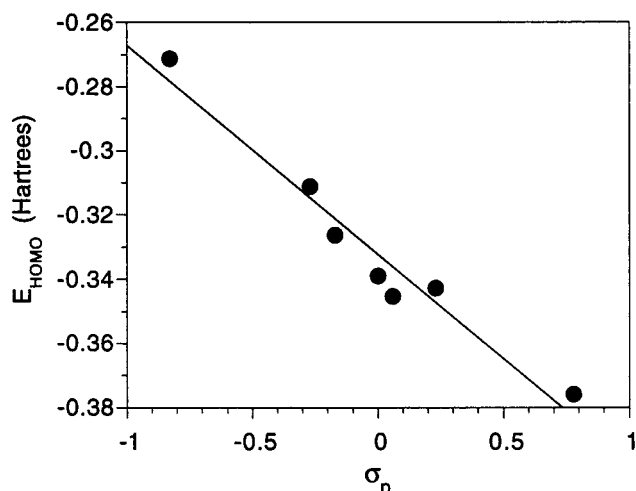


Figure 3. Plot of calculated E_{HOMO} at the HF/3-21G* level versus Hammett σ_p constants for a series of monosubstituted benzenes (X = H, F, Cl, Me, OMe, NMe₂, NO₂); $R^2 = 0.95$.

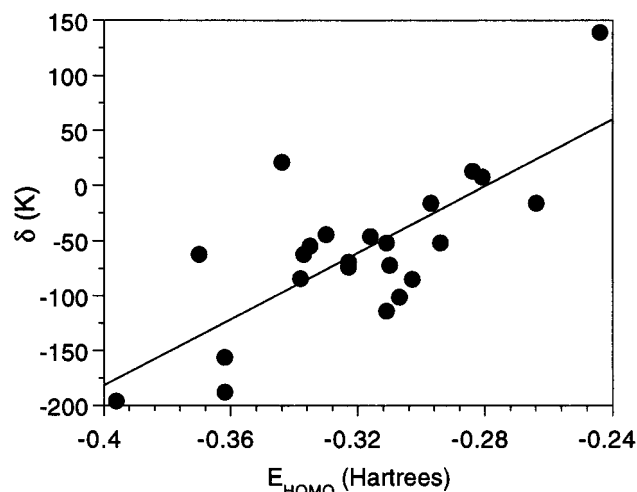


Figure 4. Plot of δ_I versus E_{HOMO} for dopants 1–6 in the nematic host 5OCB; $R^2 = 0.56$.

extreme, the electron-rich *N,N,N',N'*-tetramethylbenzidine (**1h**) raises T_{NI} by 1.4 K/mol %; at the other, the electron-poor decafluorobiphenyl (**4**) lowers T_{NI} by 2.0 K/mol %. This correlation, while statistically significant at the 99.9% confidence level,²⁷ is rather poor, which suggests that electrostatic forces do not play a predominant role in stabilizing dopant–host interactions. A better correlation was found between δ_I and α ($R^2 = 0.72$), as shown in Figure 5, which suggests that dispersion forces have a greater influence in stabilizing dopant–host interactions. Nevertheless, the data still show a considerable degree of scatter.

Taken together, the plots in Figures 4 and 5 suggest that both dispersion and electrostatic forces contribute to δ_I . To demonstrate the validity of this claim, we sought to express δ_I as a linear combination of α and E_{HOMO} according to eq 2:

$$\delta_I = a\alpha + bE_{\text{HOMO}} + c \quad (2)$$

where a , b , and c are constants which can be readily derived by multilinear regression analysis.²⁷ Such an analysis gave values of $a = 2.33 \text{ K}\cdot\text{esu}^{-1}$, $b = 756 \text{ K}\cdot\text{hartrees}^{-1}$, and $c =$

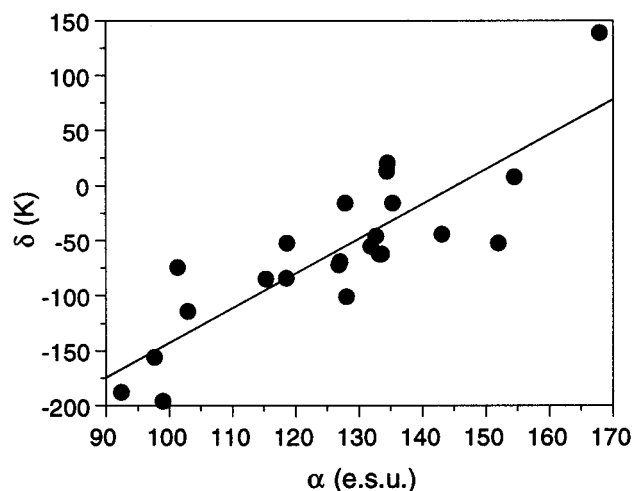


Figure 5. Plot of δ_I versus α for dopants 1–6 in the nematic host 5OCB; $R^2 = 0.72$.

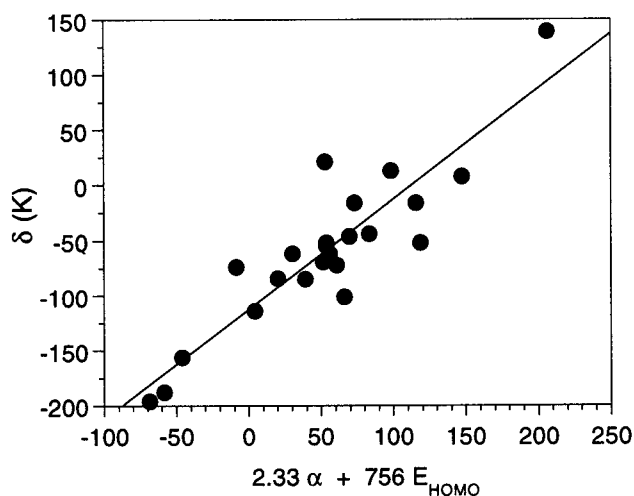


Figure 6. Plot of δ_I versus $(2.33\alpha + 756E_{\text{HOMO}})$ for dopants 1–6 in the nematic host 5OCB; $R^2 = 0.81$.

–112 K ($R^2 = 0.81$); the corresponding plot of δ_I versus $(2.33\alpha + 756E_{\text{HOMO}})$ is shown in Figure 6. The analysis shows that correlating δ_I with a linear combination of E_{HOMO} and α results in a small, yet statistically significant improvement in R^2 over that obtained by correlating δ_I with α alone.²⁸ This rather small improvement in R^2 may be due in part to the considerable collinearity between the α and E_{HOMO} values that were calculated for compounds 1–6. It is also possible, indeed likely, that other factors contributing to δ_I remain unaccounted for.

The observed correlation between E_{HOMO} and δ_I cannot be taken as evidence supporting a contribution from charge-transfer complexation; such an interpretation would be valid only if the dopants acted uniformly as electron donors with respect to the host molecules. A more valid approach to determine whether charge-transfer complexation plays a significant role in dopant–host interactions is to correlate δ_I with the smallest energy gap between the frontier molecular orbitals of the dopant and host.²⁹ As shown in Figure 7, a plot of δ_I vs dopant/host HOMO–LUMO energy gap gives a much poorer correlation ($R^2 = 0.18$) than that obtained between E_{HOMO} and δ_I (vide supra),³⁰ which

(28) The statistical significance of the improvement in R^2 was established from the partial correlation coefficient of E_{HOMO} , which was significant at the 99.9% confidence interval.^{27a} This confirms that the improvement in correlation is not merely an artifact of describing δ_I by a second variable.

(29) Fleming, I. *Frontier Molecular Orbitals and Organic Chemical Reactions*; John Wiley & Sons: New York, 1990.

(27) (a) Shorter, J. *Correlation Analysis of Organic Reactivity*; John Wiley & Sons: New York, 1982. (b) Carroll, J. D.; Green, P. E.; Chaturvedi, A. *Mathematical Tools for Applied Multivariate Analysis*; Academic Press: New York, 1997.

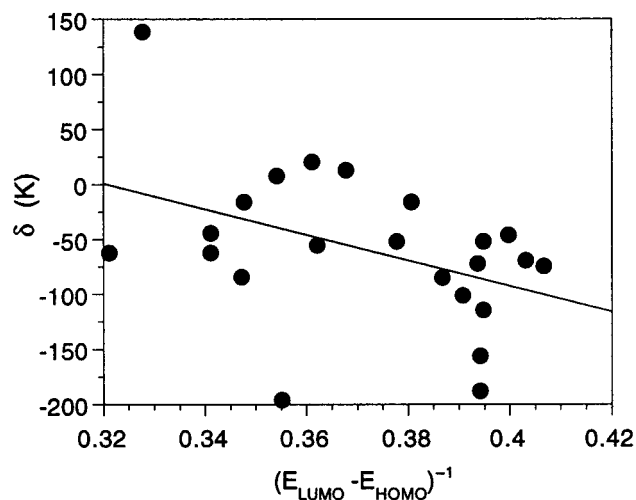


Figure 7. Plot of δ_1 versus $(E_{\text{LUMO}} - E_{\text{HOMO}})^{-1}$ for dopants **1–6** in the nematic host **5OCB**; $R^2 = 0.18$.

strongly suggests that charge-transfer complexation does not play a significant role in dopant–host interactions when compared to that played by dispersion and electrostatic forces. Other possible factors such as hardness, shape anisotropy, and polarizability anisotropy of the dopants were also examined, but they showed poorer correlations with δ_1 than either E_{HOMO} or α .

Nature of Dopant–Host Interactions. Previous studies on arene–arene interactions have shown that electron-withdrawing substituents tend to stabilize π -stacking complexes by reducing electrostatic repulsion.^{4c–e} In this study, the variation in δ_1 with respect to E_{HOMO} follows the opposite trend, which suggests that the dopants interact with the aromatic core of the nematic host predominantly in an edge-to-face orientation instead of π -stacked, with the dopant acting as hydrogen-bond acceptor.^{4f} This is consistent with X-ray diffraction studies of **5OCB** in the nematic phase.^{31,32} However, these results do not imply that arene–arene interactions are exclusively in the form of edge-to-face complexes in the nematic phase since calamitic nematic liquid crystals generally show a high degree of rotational disorder and both π -stacked and edge-to-face dopant–host geometries are expected to be significantly populated. Rather, our data suggests that edge-to-face complexes strongly influence the energetics of the dopant–host interactions.

(30) E_{HOMO} and E_{LUMO} for the nematic host **5OCB** are -0.309 and 0.083 hartrees, respectively.

(31) Bhattacharjee, B.; Paul, S.; Paul, R. *Mol. Cryst. Liq. Cryst.* **1982**, *89*, 181.

(32) Paul, S.; Mandal, P. *Mol. Cryst. Liq. Cryst.* **1985**, *131*, 223.

An interesting feature of the observed correlations is a lack of dependence on the molecular dipole moment. Since the host **5OCB** has a high longitudinal dipole moment, one might have expected unsymmetrical dopants such as **2**, **3**, and **5** to stabilize the host phase via dipole–dipole interactions and deviate from the least-squares fit in Figure 6. However, the observed deviations from the least-squares fit were found to be unrelated to molecular dipole moment. For example, the dopant with the highest molecular dipole moment (**3c**) has an intermediate δ_1 value that is in very good agreement with the least-squares fit.

One apparent anomaly is the stabilizing effect of 4,4'-dicyanobiphenyl (**1j**). It is known that nematic mesogens containing a nitrile end group tend to have considerably higher T_{NI} values than mesogens with other functionalities as end group.³³ Furthermore, crystallographic studies of **5OCB** in the solid phase have shown evidence of antiparallel dipole–dipole coupling of the nitrile groups.³² Hence, it is likely that the nitrile groups of dopant **1j** interact with the nitrile group of the nematic host in a similar fashion, which may account for the anomalously high δ_1 value measured for this dopant. It is also possible that other specific interactions between substituents on the nematic host and dopants may account for some of the scatter in Figure 6.

Summary

The effect of substituted biaryl dopants on the clearing point of a cyanobiphenyl nematic liquid crystal host were measured by differential scanning calorimetry as a function of dopant concentration for a wide range of substituents and expressed as a constant of proportionality δ_1 . Analysis of the DSC data with respect to calculated values of molecular polarizability (α) and electrostatic character of the dopant (E_{HOMO}) showed that a correlation exists between δ_1 and a linear combination of these two molecular parameters, which suggests that arene–arene interactions in the absence of a ternary solvent are strongly influenced by electrostatic as well as dispersion forces. Results of the analysis showed that dispersion forces strongly influence the stability of the phase, with a secondary influence coming from electrostatic forces. Furthermore, the results suggest that charge-transfer complexation and molecular dipole–dipole interactions do not have an appreciable effect on the stability of arene–arene interactions in the nematic phase.

Acknowledgment. We are grateful to the Natural Sciences and Engineering Research Council of Canada for financial support of this work.

JA982727H

(33) Thiemann, T.; Vill, V. *Liq. Cryst.* **1997**, *22*, 519.